A15, σ, and a Quasicrystal: Access to Complex Particle Packings via Bidisperse Diblock Copolymer Blends

Aaron P. Lindsay,† Ronald M. Lewis, III,† Bongjoon Lee,† Austin J. Peterson, † Timothy P. Lodge,†,‡ and Frank S. Bates†,*

†Department of Chemical Engineering and Materials Science and ‡Department of Chemistry, University of Minnesota, Minneapolis, Minnesota 55455, United States

ABSTRACT: A renewed focus on the phase behavior of nominally single-component, compositionally asymmetric diblock copolymers has revealed a host of previously unanticipated Frank-Kasper (FK) and quasicrystalline phases. However, these periodic and aperiodic particle packings have thus far only been reported in low molecular weight, highly conformationally asymmetric diblock copolymers, leaving researchers with a relatively small library of polymers in which these phases can be studied. In this work, we report on a simple approach to access these morphologies: blending two diblock copolymers with the same corona block length and varied core block lengths. Compositionally symmetric and asymmetric polystyrene-*b*-1,4-polybutadiene (SB) diblock copolymers with constant corona block lengths were blended together and shown via small angle X-ray scattering and transmission electron microscopy to order into the FK A15 and σ phases as well as a dodecagonal quasicrystal, providing a route to various particle packings in high molecular weight diblock copolymer melts.

Following discovery of the Frank-Kasper (FK) σ phase in a diblock copolymer melt in 2010,[1] there has been a renewed focus on the phase behavior of compositionally asymmetric diblock copolymer melts, revealing several previously unanticipated particle packings including the FK A15,[2] C14,[3,4] and C15[3,5] phases in addition to an associated dodecagonal quasicrystal (QC).[6] These complex packings, more typical of metals and their alloys, have to date been observed in several soft matter systems including multiblock polymers,[1,7–10] surfactants,[11–16] dendrimers,[17–19] colloids,[20] and giant shape amphiphiles,[21–23] suggesting universality in the packing of soft particles. However, the stability of these FK phases relative to the widely stable body-centered cubic packing (BCC) is not fully understood. In diblock copolymer melts, the emergence of these FK phases is rationalized by the tendency of micelles in an ordered melt to adopt the geometry of their respective Wigner-Seitz (WS) polyhedra, shown for BCC in Figure 1, which are on average more spherical on a FK lattice than on a BCC lattice and thus more enthalpically favorable.[24,25] However, in contrast to BCC, wherein the WS polyhedron is a truncated octahedron, FK phases require the adoption of multiple particle volumes and geometries and, as such, force polymer chains to stretch or compress to a greater extent.[25] Notably, these complex particle packings have thus far only been observed in low molecular weight ($M < 10$ kg/mol) diblock copolymers with block invariant degrees of polymerization $\bar{N}_b = N_b b^6/v^2 < 400$, where N_b is the block degree of polymerization and b is the statistical segment length calculated at a reference volume v; $\bar{N}_b$ scales as the square of the number of chains per coil volume.[26,27] This presents a challenge for the application of these nanostructures as it limits not only the length scales over which these phases can be produced, but also their possible chemistries. In this work, we show that an alternative approach, blending two diblock copolymers, facilitates access to FK phases at $\bar{N}_b > 400$, thus providing a simple route to FK phases in a much wider range of polymer systems.

Bidisperse diblock copolymer blends have been widely explored for the past four decades.[27–34] However, relatively little attention has been paid to compositionally asymmetric systems, wherein particles are the preferred nanostructure.[27,31,33,34] Koizumi et al. studied bidisperse blends of asymmetric polystyrene-*b*-1,4-polyisoprene (SI) diblock copolymers with disparate molecular weights, reporting macrophase separation into two mixed, yet distinct micelle populations when the ratio of the diblock degrees of polymerization (N_2/N_1) > 5.[31] Spontak et al. took a different approach, varying the block volume fraction $f = N_A/N$ while keeping N constant. This allowed access to a variety

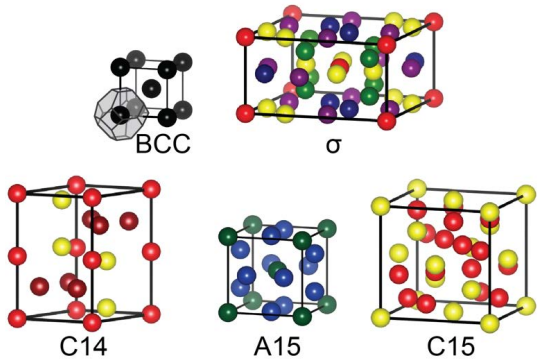

Figure 1. Periodic particle packings observed in low M diblock copolymers and predicted for bidisperse diblock copolymer blends.[1–5,35–37] Note that, to date, FK phases have not been observed for diblock copolymers with $M > 10$ kg/mol. Unit cells were constructed in Vesta.[38]

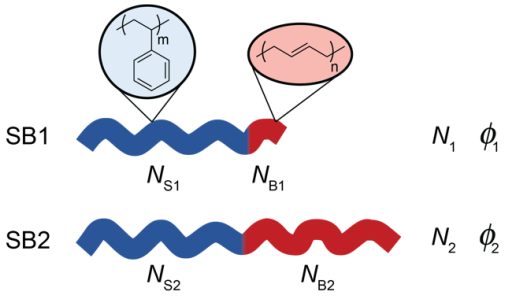

Figure 2. Polystyrene-*b*-1,4-polybutadiene (SB) chemical structure and schematic representation of the experimental SB blending

of phases, but, similar to Koizumi et al., the only periodic particle packing identified was BCC.[33] Nevertheless, in both cases an aperiodic, liquid-like packing (LLP) of micelles, referred to as a mesh phase, was observed, suggesting that either the blends precluded periodic packings or that they were kinetically trapped due to the high molecular weight of the constituent diblock copolymers. In favor of the latter, Liu et al. calculated using self-consistent mean-field theory (SCFT), which assumes $N \rightarrow \infty$, that blends of conformationally asymmetric diblock copolymers with constant N_{corona} and variable N_{core}, as well as the inverse variable N_{corona} and constant N_{core}, would afford access to the σ phase.[35] However, more recent calculations anticipate the former approach to be richer, predicting access to the A15, C14, and C15 phases in addition to σ.[36] To date, the only experimental evidence that such an approach may work is the observation of a σ phase in a blend of two low molecular weight poly(ethylene-*alt*-propylene)-*b*-poly(±-lactide) diblock copolymers with different f and N,[27] leaving unclear whether blending would work at high N or if it would allow access to other FK phases as predicted by SCFT.

In this report, we show that (1) constant N_{corona} and variable N_{core} blends facilitate access to multiple FK phases, as predicted by SCFT; (2) these phases are accessible for $\bar{N}_b > 400$; and (3) the ordering kinetics are strongly influenced by N. For this purpose, we studied blends of a symmetric and an asymmetric polystyrene-*b*-1,4,-polybutadiene (SB) diblock copolymer, both synthesized via anionic polymerization following well established procedures, wherein N_S (N_{corona}) for both polymers was kept constant and N_B (N_{core}) was varied such that $N_2/N_1 = 1.6$, as illustrated in Figure 2. We emphasize that, in a nominally single-component melt, SB does not show any evidence of a σ phase.[26] The asymmetric diblock, SB1, with $M_1 = 25$ kg/mol and $f_{B1} = 0.18$, was found via small angle X-ray scattering (SAXS) to be disordered (DIS), while the symmetric diblock, SB2, with $M_2 = 38$ kg/mol and $f_{B2} = 0.49$ had a lamellar nanostructure. Size exclusion chromatography indicated both diblock copolymers had low dispersity ($Đ \leq 1.04$). (As shown in Figure S2, SB2 had < 5 vol % residual polystyrene homopolymer leading to a negligible amount of homopolymer (< 2 vol %) in the blends of interest; see Supporting Information for additional molecular characteristics and discussion). Blends were prepared via dissolution in benzene and subsequent freeze-drying with < 0.1 wt % butylated hydroxytoluene (BHT) as an antioxidant, after which samples were hermetically sealed in aluminum pans under argon and annealed. We note that this approach resulted in no degradation over extended annealing times ($t > 60$ h) at $T \leq 180$ ºC, as evidenced by size-exclusion

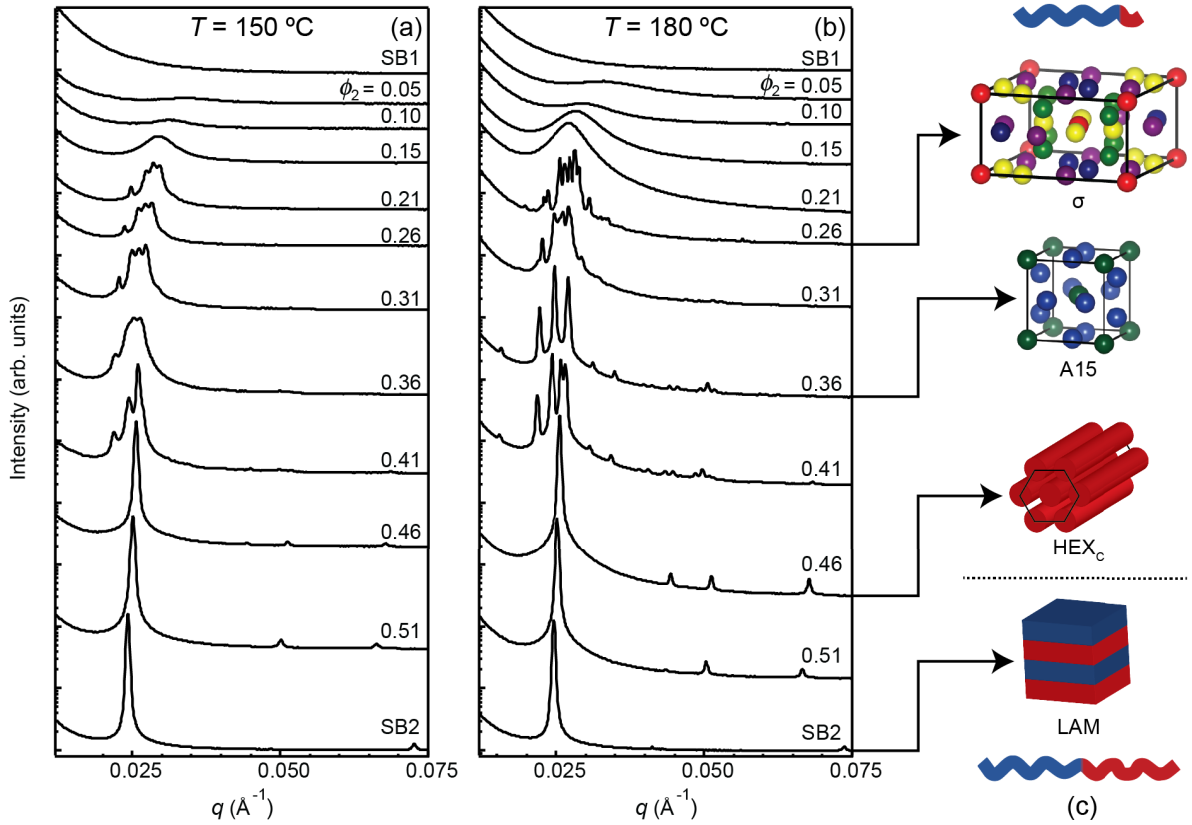

Figure 3. SAXS patterns collected following 66 and 62 h of annealing at (a) 150 and (b) 180 ºC, respectively, as well as (c) the posited equilibrium phase progression as a function of the volume fraction of the larger diblock copolymer ϕ_2.

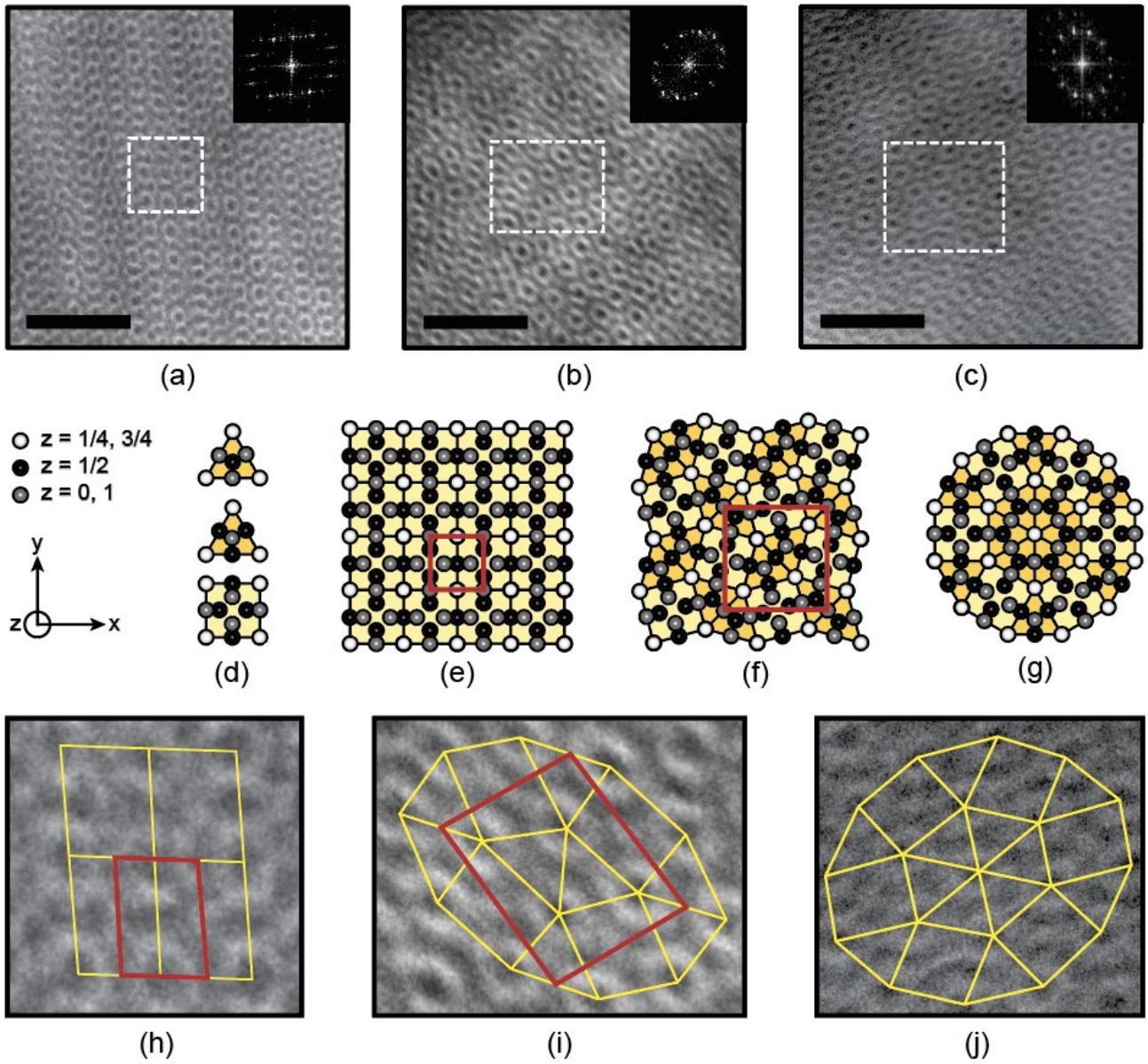

Figure 4. TEM images (a-c,h-j) and representative tilings for the observed FK A15 (a,e,h), FK σ (b,f,i), and QC (c,g,j) phases. The A15 (a,h) and QC (c,j) micrographs were obtained from blends with $\phi 2 = 0.31$ and 0.36, respectively, following 62 h of annealing at 180 ºC. The σ (b,i) micrograph was obtained following a 52 h anneal at 180 ºC with $\phi 2 = 0.26$. Tilings (e-g) are constructed using a combination of squares and equilateral triangles (shown schematically in (d) and denoted as yellow lines in (h-j)) and display the c-axis projection of each phase, analogous to the projection in the TEM images. The QC tiling shown in (g) is the characteristic dodecagonal cogwheel anticipated by a random Stampfli inflation[39] or Schlottmann rule.[40] Scale bars in (a-c) represent 200 nm and the upper right insets are Fourier transforms of the micrographs. White boxes in (a-c) are magnified in (h-j) and the FK A15 and σ unit cells are denoted by red squares (e,f,h,i).

chromatography and sample color; see the Supporting Information for more details. All samples were annealed at 180 ºC for 30 min to improve the ordering kinetics after which they were annealed at the desired temperature. Long anneals ($t \sim 60$ h) were conducted at $T = 120$, 150, and 180 ºC while intermediate points were collected on temperature ramps following 20 h of annealing at 120 ºC with approximately 30 min spent at each temperature, as shown in Figure S4. SAXS patterns were collected at certain annealing temperatures, and selected samples were quenched in liquid nitrogen to vitrify the structure, then imaged via transmission electron microscopy (TEM) as described in the Supporting Information.

As shown in Figure 3a, several SB blends developed extensive long-range order following annealing at 180 ºC, with the scattering patterns for blends with $\phi_2 = 0.26$ and 0.36 each displaying over 10 reflections with $P4_2/mnm$ or $Pm3(-)n$ symmetry corresponding to the σ and A15 phases, respectively. These observations were further supported by the characteristic $4.3.4.3^2$ and 4^4 tilings of squares and triangles clearly evident in the TEM micrographs shown in Figure 4, which correspond to the c-axis projections of the σ and A15 phases, respectively. Additionally, despite large differences in N, we observe no evidence of macrophase separation in the TEM images. As shown in Figure S9, the average particle radius calculated from SAXS scales linearly with increasing ϕ_2, further suggesting the studied blends did not macrophase separate, and in surprising agreement with predictions from strong segregation theory for a single-component melt with f and N taken as the average of those

variables in each blend (see Supporting Information). In general, at 180 ºC, we observe the sequence of phases DIS → σ → A15 → HEX_C with increasing ϕ_2 as depicted in Figure 3c. However, at ϕ_2 = 0.31, both the poorly resolved scattering pattern and the clearly discernable dodecagonal cogwheel tiling observed in the TEM micrograph shown in Figure 4j, indicate a state of σ/QC coexistence.

A dodecagonal quasicrystal is speculated to be a metastable precursor to the σ phase,[6] which is its periodic approximant. As such, observation of σ/QC coexistence at 180 ºC suggests that, even after annealing for 62 h, not all samples reached equilibrium. Although kinetic limitations are anticipated for the σ phase due to the required large-scale reorganization of particles onto a lattice with a large, low-symmetry tetragonal unit cell, the ordering times for our blends were much larger than those typically observed for low N systems away from a glass transition temperature (T_g), presenting a challenge due to the potential for sample degradation at the high required annealing temperatures. However, we can rationalize these kinetics as a consequence of slow chain exchange, required for the redistribution of mass, with the chain diffusivity for a micellar system following the relation $D = D_0\exp(-\chi N_{core})$ where χ is the Flory parameter and D_0 is the chain diffusivity in the melt.[41] Diffusivity decreases exponentially with respect to the proximity to the T_g as described by the Vogel-Fulcher-Tammann-Hesse (VFTH) equation ($D_0 \sim \exp[-\beta/(\alpha + T - T_g)]$ where α and β are constants) and has an inverse relationship with molecular weight, where $D \sim M^{-1}$ or $D \sim M^{-2.4}$ for unentangled and entangled melts, respectively.[42–45]

The temperature dependence of the ordering kinetics is especially evident as the annealing temperature approaches the T_g of polystyrene ($T_{g,S} \cong 85$ ºC; Figure S3), where, as shown in Figures 3b and Figure S10, after equivalent annealing at 150 and 120 ºC, respectively, QC and liquid-like packing (LLP) begin to dominate the particle window. This is further exacerbated as the mean segregation strength $\chi\langle N\rangle$ is increased, which occurs again with decreasing T, but also with increasing ϕ_2 as the larger diblock begins constituting a larger fraction of the blends, explaining the slower ordering kinetics of the blend with ϕ_2 = 0.31 relative to the blend with ϕ_2 = 0.26. Increasing ϕ_2 also increases $T_{ODT} - T$, which has been shown to retard ordering kinetics, eventually resulting in a kinetically trapped non-ergodic state.[6,46] However, more pertinent at 180 ºC is N. In low N ($N \sim$ 100), single-component diblock copolymer melts at higher $\chi\langle N\rangle$, but in similar proximity to a T_g, the σ phase generally emerges within a few hours,[2,6,27] in stark contrast to the ≥ 60 h required here. Keeping all else constant and assuming an entanglement degree of polymerization $N_e = N_{e,S}$ = 193, an increase in N from 100 to 371 (N for SB1) would be associated with a roughly 26 fold increase in the longest relaxation time τ [$\tau_{SB}/\tau_{IL} \sim N_{SB}^3/(N_e N_{IL}^2)$], in reasonable agreement with the roughly 20 fold increase in the ordering time. This is certainly an oversimplification for these diblock copolymer blends, where the rate of chain exchange will differ for the two polymers and dynamics differ between blocks. Nevertheless it illustrates some of the challenges associated with obtaining FK phases at high N and, while proximity to the T_g and the segregation strength can generally be adapted for a given system, this N-dependence of the ordering kinetics will likely impose an upper limit on the length scales over which FK phases can be observed in traditional diblock copolymers.

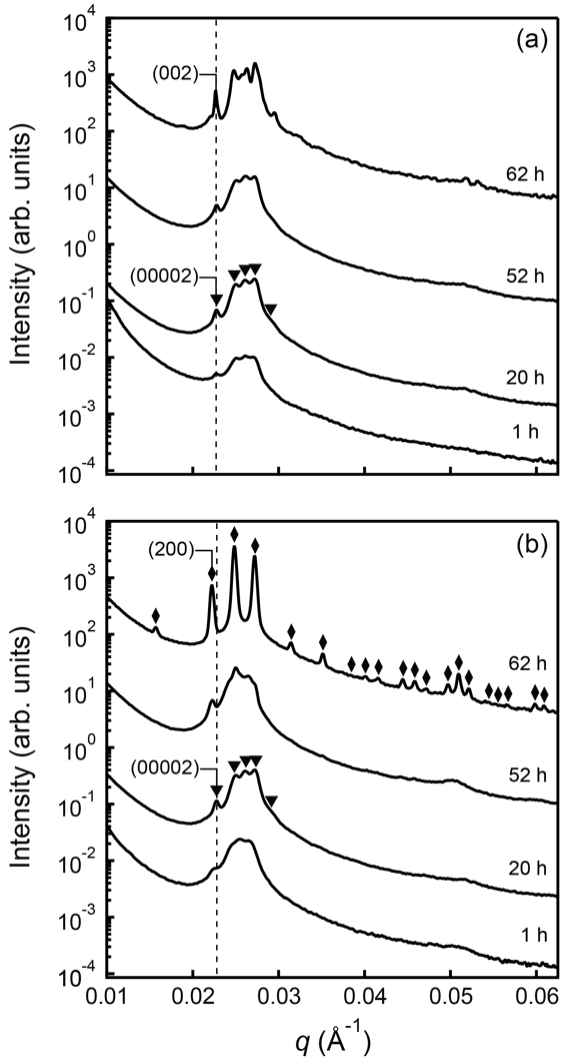

Figure 5. Vertically shifted 1D SAXS patterns collected at 180 ºC as a function of time for samples with ϕ_2 = 0.31 (a) and 0.36 (b). Diamonds and inverted triangles denote scattering reflections corresponding to A15 and QC packings, respectively. The dashed lines in (a) and (b) denote the QC (00002) scattering reflection. Note that the 62 h patterns were collected from separate specimens prepared from the same blend batch.

Unlike periodic FK phases, aperiodic packings emerge rapidly. As shown in Figures 5a and 5b for blends with ϕ_2 = 0.31 and 0.36, respectively, the QC (00002) reflection can be clearly observed within 1 h at 180 ºC and well-resolved patterns emerge in less than a day. These QC packings persist for ~30 h at which point the σ and A15 phases begin to emerge. However, a notable difference can be observed between the σ and A15-forming blends. As shown in Figures 5a and 5b, whereas the transition from a QC to a σ phase results in only modest disruption of the scattering pattern, with the (00002) of the QC remaining at the same q value as the (002) of the σ phase, the QC (00002) peak shifts from 0.0225 Å^{-1} to 0.0220 Å^{-1} as it transitions to the (200) peak of the A15 phase. We note that these reflections all correspond to the spacing between densely packed planes. Therefore, the increased spacing for A15 implies that there is an increase in the mean aggregation number, which we estimate to be roughly 12% as detailed in the Supporting Information. This result suggests that the emergence of A15 from the QC is enthalpically driven, as an increase in particle size is associated with

a decrease in the interfacial area per chain. Intriguingly, despite the change in aggregation number and the higher $\chi\langle N\rangle$ of the A15-forming blend, A15 orders more quickly than σ in a lower $\chi\langle N\rangle$ blend, suggesting that the higher symmetry and smaller size of the A15 unit cell relative to σ dramatically improves the ordering kinetics. Further, we note that, as shown in Figure S11, the ordering kinetics can be even further improved when A15 is in coexistence with HEX_C, a result we attribute to bypassing the QC, as also detailed in the Supporting Information.

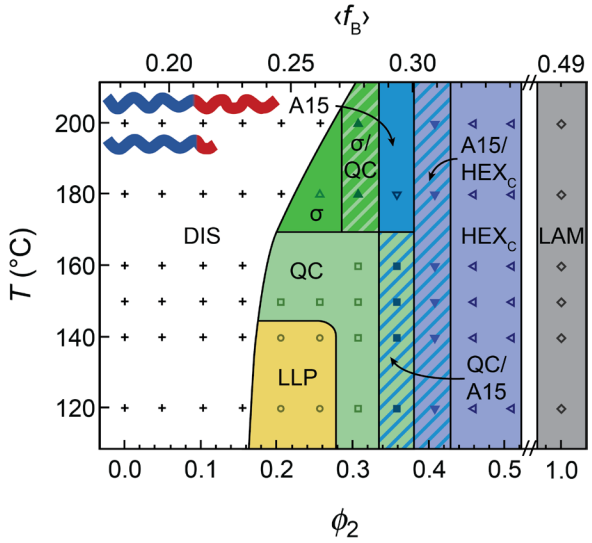

Figure 6. Experimental phase diagram for blends of SB1 and SB2. DIS, LLP, QC, HEX_C, and LAM denote disorder, liquid-like packing, a dodecagonal quasicrystal, hexagonally-packed cylinders, and lamellae, respectively. Phase assignments at 120, 150, and 180 ºC reflect the phase behavior observed after long annealing times with intermediate assignments determined from scattering patterns collected on a temperature ramp with 30 min of annealing at each temperature, as shown in Figure S4. A striped background indicates phase coexistence with the phase listed first being the dominant phase. The schematic in the upper left corner displays the difference in the lengths of SB1 and SB2.

Despite the kinetic challenges outlined above, the blending approach taken here enabled access for the first time to the FK A15 and σ phases at high N, with slow kinetics facilitating formation of the metastable QC packing. As shown in Figure 6, and noted earlier, the equilibrium phase progression at 180 ºC largely proceeds with increasing ϕ_2 or $\langle f_B\rangle$ from DIS to σ to A15 and then to HEX_C with intermediate A15/HEX_C coexistence. This agrees qualitatively with SCFT predictions, with differences in f_{B1} and conformational asymmetry shifting the phase progression relative to SCFT calculations in ϕ_2 and N_2/N_1, respectively.[36] However, the FK C14 and C15 phases predicted by SCFT are absent from the experimental phase portrait.[36] We speculate this is due to the low molecular weight of SB1 resulting in disorder at low ϕ_2. Nonetheless, in line with predictions from SCFT, we can rationalize the stabilization of the FK A15 and σ phases over BCC in the blends as stemming primarily from increased interfacial curvature and preferential segregation of diblock copolymers.[35]

As can be seen in Figure 6, the sphere-cylinder OOT occurs at a higher composition than occurs in the nominally single-component melt,[26] shifting from $f_B \approx 0.20$ to $\langle f_B\rangle \approx 0.31$ due to the high asymmetry of SB1, which drives interfacial curvature in the studied blends. At higher minority block compositions, the core is larger and thus the enthalpic benefit of the more spherical FK phases stabilizes them over BCC.[25] However, even without this increased curvature, preferential segregation of SB1 and SB2 to regions of higher and lower curvature, respectively, as predicted by SCFT, reduces the chain stretching penalties associated with the variations in particle size and geometry required by FK phases.[35] When coupled with the constraint of constant corona block length, this effect likely also drives increased polyhedral warping of the core due to the need to maintain constant coronal density and the shorter length of SB1, again increasing interfacial area. We note that, aside from this reduction in chain stretching afforded by blending, these effects are analogous to what is anticipated at high conformational asymmetry, where differences in the pervaded volume of each block drive interfacial curvature and an imbalance in block stretching penalties drive polyhedral warping at finite N.[25,47] However, notably, the blending approach taken here is presumably applicable over a much wider range of length scales and polymer chemistries. Lastly, we rationalize the emergence of the A15 phase at $\langle f_B\rangle$ greater than σ as a consequence of the higher chain stretching penalties associated with the σ phase, which we anticipate are further exacerbated as the core begins to impinge on the corona.[25]

In summary, we have shown that blending asymmetric and symmetric SB diblock copolymers with constant N_{corona} and variable N_{core} affords access to the FK σ and A15 phases, in addition to a QC. Notably, this represents the first report of FK and QC packings in a diblock copolymer system with $M > 10$ kg/mol. Further, this approach does not require high χ, or highly conformationally asymmetric diblock copolymers, and could potentially facilitate access to complex particle packings in a substantially wider range of polymers and over a wider range of length scales. We note that the upper length scale at which these phases can be produced will be limited by the ordering kinetics at high N, potentially explaining the LLP (referred to as a mesh phase) observed in past SI blends.[31,33] However, we anticipate that this upper limit can be expanded by blending diblock copolymers with more facile kinetics such as those with bottlebrush architectures,[48] making the application of soft FK and QC packings in fields ranging from lithography to photonics even more promising

ASSOCIATED CONTENT

Supporting Information

The Supporting Information is available free of charge on the ACS Publications website.

Experimental details and additional characterization data (PDF)

AUTHOR INFORMATION

Corresponding Author

* E-mail: bates001@umn.edu

ORCID

Aaron P. Lindsay: 0000-0003-0223-193X

Ronald M. Lewis, III: 0000-0002-7388-4439

Bongjoon Lee: 0000-0001-6318-2014

Austin J. Peterson: 0000-0001-8818-1333

Timothy P. Lodge: 0000-0001-5916-8834

Frank S. Bates: 0000-0003-3977-1278

Notes

The authors declare no competing financial interest.

ACKNOWLEDGMENT

Support for this work was provided by the National Science Foundation under Grant No. DMR-1801993 as well as the National Science Foundation Graduate Research Fellowship under Grant No. 00039202. SAXS experiments were conducted at the Advanced Photon Source (APS), Sector 5 (DuPont-Northwestern-Dow Collaborative Access Team, DND-CAT). DND-CAT is supported by E.I. DuPont de Nemours & Co., The Dow Chemical Company, and Northwestern University. Use of the APS, an Office of Science User Facility operated for the U.S. Department of Energy (DOE) Office of Science by Argonne National Laboratory, was supported by the U.S. DOE under Contract No. DE-AC02-06CH11357. SAXS data was collected using an instrument funded by the National Science Foundation under Grant No. 0960140. Parts of this work were carried out in the Characterization Facility at the University of Minnesota, which receives partial support from the NSF through the MRSEC program.

REFERENCES

(1) Lee, S.; Bluemle, M. J.; Bates, F. S. Discovery of a Frank-Kasper σ Phase in Sphere-Forming Block Copolymer Melts. *Science* **2010**, *330*, 349–353. https://doi.org/10.1126/science.1195552.

(2) Bates, M. W.; Lequieu, J.; Barbon, S. M.; Lewis, R. M.; Delaney, K. T.; Anastasaki, A.; Hawker, C. J.; Fredrickson, G. H.; Bates, C. M. Stability of the A15 Phase in Diblock Copolymer Melts. *Proc. Natl. Acad. Sci. U. S. A.* **2019**, *116*, 13194–13199. https://doi.org/10.1073/pnas.1900121116.

(3) Kim, K.; Schulze, M. W.; Arora, A.; Lewis, R. M.; Hillmyer, M. A.; Dorfman, K. D.; Bates, F. S. Thermal Processing of Diblock Copolymer Melts Mimics Metallurgy. *Science* **2017**, *356*, 520–523. https://doi.org/10.1126/science.aam7212.

(4) Jeon, S.; Jun, T.; Jo, S.; Ahn, H.; Lee, S.; Lee, B.; Ryu, D. Y. Frank–Kasper Phases Identified in PDMS- b -PTFEA Copolymers with High Conformational Asymmetry. *Macromol. Rapid Commun.* **2019**, *40*, 1900259. https://doi.org/10.1002/marc.201900259.

(5) Uddin, M. H.; Rodriguez, C.; López-Quintela, A.; Leisner, D.; Solans, C.; Esquena, J.; Kunieda, H. Phase Behavior and Microstructure of Poly(Oxyethylene)−Poly(Dimethylsiloxane) Copolymer Melt. *Macromolecules* **2003**, *36*, 1261–1271. https://doi.org/10.1021/ma0210978.

(6) Gillard, T. M.; Lee, S.; Bates, F. S. Dodecagonal Quasicrystalline Order in a Diblock Copolymer Melt. *Proc. Natl. Acad. Sci. U. S. A.* **2016**, *113*, 5167–5172. https://doi.org/10.1073/pnas.1601692113.

(7) Zhang, J.; Bates, F. S. Dodecagonal Quasicrystalline Morphology in a Poly(Styrene-*b*-Isoprene-*b*-Styrene-*b*-Ethylene Oxide) Tetrablock Terpolymer. *J. Am. Chem. Soc.* **2012**, *134*, 7636–7639. https://doi.org/10.1021/ja301770v.

(8) Miyamori, Y.; Suzuki, J.; Takano, A.; Matsushita, Y. Periodic and Aperiodic Tiling Patterns from a Tetrablock Terpolymer System of the A_1BA_2C Type. *ACS Macro Lett.* **2020**, *9*, 32–37. https://doi.org/10.1021/acsmacrolett.9b00861.

(9) Takano, A.; Kawashima, W.; Noro, A.; Isono, Y.; Tanaka, N.; Dotera, T.; Matsushita, Y. A Mesoscopic Archimedean Tiling Having a New Complexity in an ABC Star Polymer. *J. Polym. Sci. Part B Polym. Phys.* **2005**, *43*, 2427–2432. https://doi.org/10.1002/polb.20537.

(10) Hayashida, K.; Dotera, T.; Takano, A.; Matsushita, Y. Polymeric Quasicrystal: Mesoscopic Quasicrystalline Tiling in ABC Star Polymers. *Phys. Rev. Lett.* **2007**, *98*, 195502. https://doi.org/10.1103/PhysRevLett.98.195502.

(11) Jayaraman, A.; Mahanthappa, M. K. Counterion-Dependent Access to Low-Symmetry Lyotropic Sphere Packings of Ionic Surfactant Micelles. *Langmuir* **2018**, *34*, 2290–2301. https://doi.org/10.1021/acs.langmuir.7b03833.

(12) Baez-Cotto, C. M.; Mahanthappa, M. K. Micellar Mimicry of Intermetallic C14 and C15 Laves Phases by Aqueous Lyotropic Self-Assembly. *ACS Nano* **2018**, *12*, 3226–3234. https://doi.org/10.1021/acsnano.7b07475.

(13) Kim, S. A.; Jeong, K. J.; Yethiraj, A.; Mahanthappa, M. K. Low-Symmetry Sphere Packings of Simple Surfactant Micelles Induced by Ionic Sphericity. *Proc. Natl. Acad. Sci. U. S. A.* **2017**, *114*, 4072–4077. https://doi.org/10.1073/pnas.1701608114.

(14) Luzzati, V.; Vargas, R.; Gulik, A.; Mariani, P.; Seddon, J. M.; Rivas, E. Lipid Polymorphism: A Correction. The Structure of the Cubic Phase of Extinction Symbol Fd--Consists of Two Types of Disjointed Reverse Micelles Embedded in a Three-Dimensional Hydrocarbon Matrix. *Biochemistry* **1992**, *31*, 279–285. https://doi.org/10.1021/bi00116a038.

(15) Vargas, R.; Mariani, P.; Gulik, A.; Luzzati, V. Cubic Phases of Lipid-Containing Systems. The Structure of Phase Q223 (Space Group Pm3n). An X-Ray Scattering Study. *J. Mol. Biol.* **1992**, *225*, 137–145. https://doi.org/10.1016/0022-2836(92)91031-J.

(16) Seddon, J. M.; Zeb, N.; Templer, R. H.; McElhaney, R. N.; Mannock, D. A. An *Fd3m* Lyotropic Cubic Phase in a Binary Glycolipid/Water System. *Langmuir* **1996**, *12*, 5250–5253. https://doi.org/10.1021/la960664f.

(17) Percec, V.; Ahn, C. H.; Ungar, G.; Yeardley, D. J. P.; Möller, M.; Sheiko, S. S. Controlling Polymer Shape through the Self-Assembly of Dendritic Side- Groups. *Nature* **1998**, *391*, 161–164. https://doi.org/10.1038/34384.

(18) Zeng, X.; Ungar, G.; Liu, Y.; Percec, V.; Dulcey, A. E.; Hobbs, J. K. Supramolecular Dendritic Liquid Quasicrystals. *Nature* **2004**, *428*, 157–160. https://doi.org/10.1038/nature02368.

(19) Hudson, S. D.; Jung, H. T.; Percec, V.; Cho, W. D.; Johansson, G.; Ungar, G.; Balagurusamy, V. S. K. Direct Visualization of Individual Cylindrical and Spherical Supramolecular Dendrimers. *Science* **1997**, *278*, 449–452. https://doi.org/10.1126/science.278.5337.449.

(20) Fischer, S.; Exner, A.; Zielske, K.; Perlich, J.; Deloudi, S.; Steurer, W.; Lindner, P.; Förster, S. Colloidal Quasicrystals with 12-Fold and 18-Fold Diffraction Symmetry. *Proc. Natl. Acad. Sci. U. S. A.* **2011**, *108*, 1810–1814. https://doi.org/10.1073/pnas.1008695108.

(21) Su, Z.; Hsu, C. H.; Gong, Z.; Feng, X.; Huang, J.; Zhang, R.; Wang, Y.; Mao, J.; Wesdemiotis, C.; Li, T.; et al. Identification of a Frank–Kasper Z Phase from Shape Amphiphile Self-Assembly. *Nat. Chem.* **2019**, *11*, 899–905. https://doi.org/10.1038/s41557-019-0330-x.

(22) Yue, K.; Huang, M.; Marson, R. L.; Hec, J.; Huang, J.; Zhou, Z.; Wang, J.; Liu, C.; Yan, X.; Wu, K.; et al. Geometry Induced Sequence of Nanoscale Frank-Kasper and Quasicrystal Mesophases in Giant Surfactants. *Proc. Natl. Acad. Sci. U. S. A.* **2016**, *113*, 14195–14200. https://doi.org/10.1073/pnas.1609422113.

(23) Huang, M.; Hsu, C. H.; Wang, J.; Mei, S.; Dong, X.; Li, Y.; Li, M.; Liu, H.; Zhang, W.; Aida, T.; et al. Selective Assemblies of Giant Tetrahedra via Precisely Controlled Positional Interactions. *Science* **2015**, *348*, 424–428. https://doi.org/10.1126/science.aaa2421.

(24) Lee, S.; Leighton, C.; Bates, F. S. Sphericity and Symmetry Breaking in the Formation of Frank-Kasper Phases from One Component Materials. *Proc. Natl. Acad. Sci. U. S. A.* **2014**, *111*, 17723–17731. https://doi.org/10.1073/pnas.1408678111.

(25) Reddy, A.; Buckley, M. B.; Arora, A.; Bates, F. S.; Dorfman, K. D.; Grason, G. M. Stable Frank-Kasper Phases of Self-Assembled, Soft Matter Spheres. *Proc. Natl. Acad. Sci. U. S. A.* **2018**, *115*, 10233–10238. https://doi.org/10.1073/pnas.1809655115.

(26) Lewis, R. M.; Arora, A.; Beech, H. K.; Lee, B.; Lindsay, A. P.; Lodge, T. P.; Dorfman, K. D.; Bates, F. S. Role of Chain Length in the Formation of Frank-Kasper Phases in Diblock Copolymers. *Phys. Rev. Lett.* **2018**, *121*, 208002. https://doi.org/10.1103/PhysRevLett.121.208002.

(27) Schulze, M. W.; Lewis, R. M.; Lettow, J. H.; Hickey, R. J.; Gillard, T. M.; Hillmyer, M. A.; Bates, F. S. Conformational Asymmetry and Quasicrystal Approximants in Linear Diblock Copolymers. *Phys. Rev. Lett.* **2017**, *118*, 207801. https://doi.org/10.1103/PhysRevLett.118.207801.

(28) Hadziioannou, G.; Skoulios, A.; Hadziioannou, G. Structural

Study of Mixtures of Styrene/Isoprene Two- and Three-Block Copolymers. *Macromolecules* **1982**, *15*, 267–271. https://doi.org/10.1021/ma00230a013.

(29) Hashimoto, T.; Yamasaki, K.; Koizumi, S.; Hasegawa, H. Ordered Structure in Blends of Block Copolymers. 1. Miscibility Criterion for Lamellar Block Copolymers. *Macromolecules* **1993**, *26*, 2895–2904. https://doi.org/10.1021/ma00063a039.

(30) Hashimoto, T.; Koizumi, S.; Hasegawa, H. Ordered Structure in Blends of Block Copolymers.2. Self-Assembly for Immiscible Lamella-Forming Copolymers. *Macromolecules* **1994**, *27*, 1562–1570. https://doi.org/10.1021/ma00084a043.

(31) Koizumi, S.; Hasegawa, H.; Hashimoto, T. Ordered Structure in Blends of Block Copolymers. 3. Self-Assembly in Blends of Sphere- or Cylinder-Forming Copolymers. *Macromolecules* **1994**, *27*, 4371–4381. https://doi.org/10.1021/ma00093a044.

(32) Vilesov, A. D.; Floudas, G.; Pakula, T.; Melenevskaya, E. Y.; Birshtein, T. M.; Lyatskaya, Y. V. Lamellar Structure Formation in the Mixture of Two Cylinder-forming Block Copolymers. *Macromol. Chem. Phys.* **1994**, *195*, 2317–2326. https://doi.org/10.1002/macp.1994.021950704.

(33) Spontak, R. J.; Fung, J. C.; Braunfeld, M. B.; Sedat, J. W.; Agard, D. A.; Kane, L.; Smith, S. D.; Satkowski, M. M.; Ashraf, A.; Hajduk, D. A.; et al. Phase Behavior of Ordered Diblock Copolymer Blends: Effect of Compositional Heterogeneity. *Macromolecules* **1996**, *29*, 4494–4507. https://doi.org/10.1021/ma9515689.

(34) Court, F.; Hashimoto, T. Morphological Studies of Binary Mixtures of Block Copolymers. 1. Cosurfactant Effects and Composition Dependence of Morphology. *Macromolecules* **2001**, *34*, 2536–2545. https://doi.org/10.1021/MA001314+.

(35) Liu, M.; Qiang, Y.; Li, W.; Qiu, F.; Shi, A. C. Stabilizing the Frank-Kasper Phases via Binary Blends of AB Diblock Copolymers. *ACS Macro Lett.* **2016**, *5*, 1167–1171. https://doi.org/10.1021/acsmacrolett.6b00685.

(36) Kim, K.; Arora, A.; Lewis, R. M.; Liu, M.; Li, W.; Shi, A. C.; Dorfman, K. D.; Bates, F. S. Origins of Low-Symmetry Phases in Asymmetric Diblock Copolymer Melts. *Proc. Natl. Acad. Sci. U. S. A.* **2018**, *115*, 847–854. https://doi.org/10.1073/pnas.1717850115.

(37) Bates, F. S.; Cohen, R. E.; Berney, C. V. Small-Angle Neutron Scattering Determination of Macrolattice Structure in a Polystyrene-Polybutadiene Diblock Copolymer. *Macromolecules* **1982**, *15*, 589–592. https://doi.org/10.1021/ma00230a073.

(38) Momma, K.; Izumi, F. VESTA 3 for Three-Dimensional Visualization of Crystal, Volumetric and Morphology Data. *J. Appl. Crystallogr.* **2011**, *44*, 1272–1276. https://doi.org/10.1107/S0021889811038970.

(39) Stampfli, P. A Dodecagonal Quasi-Periodic Lattice in 2 Dimensions. *Helv. Phys. Acta* **1986**, *59*, 1260–1263.

(40) Baake, M.; Klitzing, R.; Schlottmann, M. Fractally Shaped Acceptance Domains of Quasiperiodic Square-Triangle Tilings with Dedecagonal Symmetry. *Phys. A Stat. Mech. its Appl.* **1992**, *191*, 554–558. https://doi.org/10.1016/0378-4371(92)90582-B.

(41) Cavicchi, K. A.; Lodge, T. P. Self-Diffusion and Tracer Diffusion in Sphere-Forming Block Copolymers. *Macromolecules* **2003**, *36*, 7158–7164. https://doi.org/10.1021/ma0346815.

(42) Vogel, H. The Law of the Relation between the Viscosity of Liquids and the Temperature. *Phys. Zeitschrift* **1921**, *22*, 645–646.

(43) Fulcher, G. S. Analysis of Recent Measurements of the Viscosity of Glasses. *J. Am. Ceram. Soc.* **1925**, *8*, 339–355.

(44) Tamman, G.; Hesse, W. Die Abhängigkeit Der Viscosität von Der Temperatur Bie Unterkühlten Flüssigkeiten. *Zeitschrift für Anorg. und Allg. Chemie* **1926**, *156*, 245–257.

(45) Berry, G. C.; Fox, T. G. The Viscosity of Polymers and Their Concentrated Solutions. *Adv. Polym. Sci* **1968**, *5*, 261–357.

(46) Lewis, R. M.; Beech, H. K.; Jackson, G. L.; Maher, M. J.; Kim, K.; Narayanan, S.; Lodge, T. P.; Mahanthappa, M. K.; Bates, F. S. Dynamics of a Supercooled Disordered Sphere-Forming Diblock Copolymer as Determined by X-Ray Photon Correlation and Dynamic Mechanical Spectroscopies. *ACS Macro Lett.* **2018**, *7*, 1486–1491. https://doi.org/10.1021/acsmacrolett.8b00740.

(47) Xie, N.; Li, W.; Qiu, F.; Shi, A. C. σ Phase Formed in Conformationally Asymmetric AB-Type Block Copolymers. *ACS Macro Lett.* **2014**, *3*, 909–910. https://doi.org/10.1021/mz500445v.

(48) Sveinbjörnsson, B. R.; Weitekamp, R. A.; Miyake, G. M.; Xia, Y.; Atwater, H. A.; Grubbs, R. H. Rapid Self-Assembly of Brush Block Copolymers to Photonic Crystals. *Proc. Natl. Acad. Sci. U. S. A.* **2012**, *109*, 14332–14336. https://doi.org/10.1073/pnas.1213055109.

TOC Graphic